

## Enhancement of spontaneous recombination rate in a quantum well by resonant surface plasmon coupling

Arup Neogi,\* Chang-Won Lee, and Henry O. Everitt

*Department of Physics, Duke University, Durham, North Carolina 27708*

Takamasa Kuroda and Atsushi Tackeuchi

*Department of Applied Physics, Waseda University, Okubo 3-4-1, Shinjuku, Tokyo 169-8555, Japan*

Eli Yablonovitch

*Department of Electrical Engineering, University of California, Los Angeles, California 90095*

(Received 28 June 2002; published 4 October 2002)

Using time-resolved photoluminescence measurements, the recombination rate in an  $\text{In}_{0.18}\text{Ga}_{0.82}\text{N}/\text{GaN}$  quantum well (QW) is shown to be greatly enhanced when spontaneous emission is resonantly coupled to a silver surface plasmon. The rate of enhanced spontaneous emission into the surface plasmon was as much as 92 times faster than QW spontaneous emission into free space. A calculation, based on Fermi's golden rule, reveals that the enhancement is very sensitive to silver thickness and indicates even greater enhancements are possible for QW's placed closer to the surface metal coating.

DOI: 10.1103/PhysRevB.66.153305

PACS number(s): 78.47.+p, 42.50.Ct, 73.20.Mf, 78.55.Cr

The spontaneous emission (SE) decay constant  $\tau$  for radiating dipoles at  $\vec{r}_e$  is given by Fermi's golden rule

$$\frac{1}{\tau} = \frac{2\pi}{\hbar} |\langle f | \vec{d} \cdot \vec{E}(\vec{r}_e) | i \rangle|^2 \rho(\hbar\omega), \quad (1)$$

where  $\rho(\hbar\omega)$  is the photon density of states (DOS) and  $\langle f | \vec{d} \cdot \vec{E}(\vec{r}_e) | i \rangle$  is the dipole emission matrix element. As pointed out by Purcell, SE may be enhanced by altering the photon DOS.<sup>1</sup> For example, the ratio of enhanced to free space emission (the Purcell factor  $F$ ) has been measured to be as large as 5 in an atomic system by placing the radiating atoms in a high  $Q$ , low volume cavity.<sup>2,3</sup> A Purcell factor of up to 6 has been observed from quantum well (QW) and quantum dot emitters in vertical cavity surface emitting laser structures, while an enhancement of 15 has been observed from quantum dots in a microdisk cavity.<sup>4,5</sup> Photonic crystals and distributed Bragg gratings have also been used to enhance the SE rate by as much as a factor of 4.5.<sup>6-8</sup> Such enhanced SE rates, achieved by increasing the photonic DOS in a small cavity, permit lower threshold, higher modulation frequency lasers as well as more efficient light emitting diodes.

The SE rate can also be modified when semiconductor or dye emitters are coupled to a surface plasmon (SP) of a metallic film.<sup>9-12</sup> A single QW can experience strong quantum electrodynamic coupling to a SP mode if placed within the SP fringing field penetration depth. An electron-hole pair in the QW recombines and emits a photon into a SP mode instead of into free space. The degree of SE rate modification for a given wavelength depends on the SP DOS at that wavelength. The strongest enhancement occurs near the asymptotic limit of the SP dispersion branch, the SP "resonance" energy  $E_{sp}$ , where the SP DOS is very high. Non-resonant, SP-mediated SE enhancements as large as 6 have been observed from GaAs QW's near thin Ag films.<sup>9</sup> Even greater enhancements are possible for wide band-gap semi-

conductors whose emission wavelength is coincident with  $E_{sp}$ . In this report, time-resolved photoluminescence (TRPL) measurements of a partially silver-coated  $\text{InGaN}/\text{GaN}$  QW directly demonstrate the SP-mediated resonant enhancement of the recombination rate in a semiconductor QW.

An  $\text{InGaN}/\text{GaN}$  QW was used in these experiments, grown by metal-organic chemical vapor deposition on sapphire substrate.<sup>13</sup> Over a 1.5- $\mu\text{m}$  Si-doped GaN buffer layer was grown a 28-nm  $\text{In}_{0.04}\text{Ga}_{0.96}\text{N}$  reference layer, a 6-nm GaN layer, and the 3-nm  $\text{In}_{0.18}\text{Ga}_{0.82}\text{N}$  QW as shown in Fig. 1. Above the QW was a 12-nm Si-doped GaN cap layer, placing the QW within the fringing field depth of the SP. A layer of silver,  $\sim 8$  nm thick, was deposited by electron beam evaporation on one half of the sample surface. The other half was left bare to facilitate direct comparison of the silvered and unsilvered results.

The bulk plasmon energy of silver is 3.76 eV, but the SP energy of Ag is lowered by the GaN dielectric constant.<sup>14</sup>

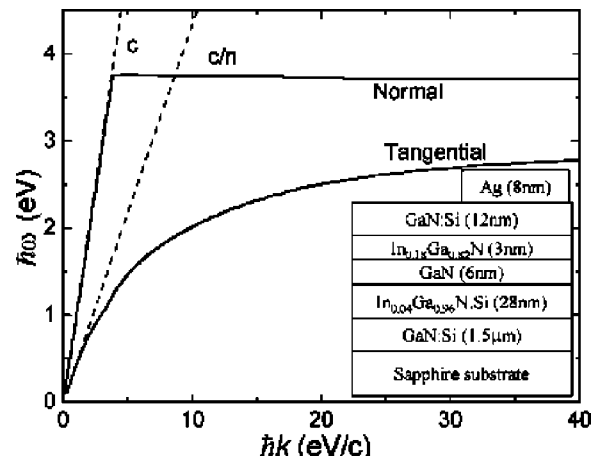


FIG. 1. The calculated surface plasmon dispersion relation for tangential and normal modes. Inset: The structure of the sample studied.

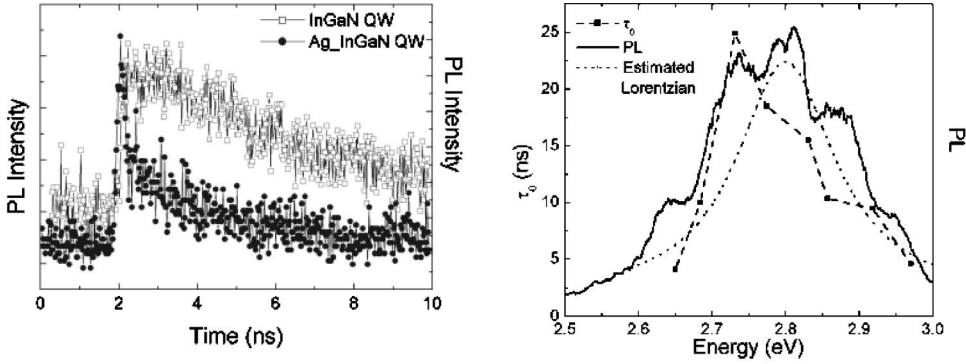


FIG. 2. (a) TRPL decay of the unsilvered and silvered InGaN QW for a 25-nm-wide wavelength detection window (2.79–2.96 eV), with pump energy of 3.14 eV. (b) Comparison of the time-integrated PL and the TRPL-measured recombination rate constant ( $\tau_0$ ) of the unsilvered InGaN QW. The dashed curve is the estimation given by Eq. (4) with  $\hbar\omega_c = 2.8$  eV and  $\hbar\Delta\omega = 0.16$  eV.

The SP dispersion relation is derived, using Maxwell's equations, from the known dielectric properties of Ag and GaN.<sup>15</sup> Considering a silver film of thickness  $t$  and permittivity  $\epsilon_2$ , sandwiched between GaN and air with permittivities  $\epsilon_1$  and  $\epsilon_3$  respectively, the boundary condition gives the SP dispersion relation

$$\left(\frac{\gamma_1}{\epsilon_1} + \frac{\gamma_2}{\epsilon_2}\right)\left(\frac{\gamma_3}{\epsilon_3} + \frac{\gamma_2}{\epsilon_2}\right) - \left(\frac{\gamma_1}{\epsilon_1} - \frac{\gamma_2}{\epsilon_2}\right)\left(\frac{\gamma_3}{\epsilon_3} - \frac{\gamma_2}{\epsilon_2}\right)e^{-2\gamma_2 t} = 0, \quad (2)$$

where  $\gamma_i = k^2 - \epsilon_i \omega^2 / c^2$ ,  $i = 1, 2, 3$ , and  $k = 2\pi/\lambda$  is the wave vector. The SP dispersion contains tangential and normal-mode branches (Fig. 1), indicating the dominant direction of current flow in the silver film. For silver films with  $t \geq 8$  nm, the tangential SP branch asymptotically approaches  $E_{sp} = 2.85$  eV ( $\lambda_{sp} = 436$  nm), the SP “resonance” energy. Because the photon DOS is proportional to  $dk/d\omega$ , the SP DOS and SE enhancement will be greatest at the SP resonance.

The resonant enhancement is measured by comparing the luminescence decay rate from the photoexcited QW on the silvered and unsilvered sides. Room-temperature TRPL measurements were performed using a 100-MHz Kerr-lens mode-locked, frequency-doubled Ti:sapphire (Ti:S) laser with average incident pump power of 10 mW ( $\sim 13 \mu\text{J}/\text{cm}^2$ ). The pump excitation energy (3.14 eV or 395 nm) was chosen to be below the band gap of the InGaN reference layer and GaN layers so electron-hole pairs were generated only in the QW. However, defects in the Si:GaN may also emit. The luminescence signal was dispersed in a grating spectrometer (600 g/mm) and measured simultaneously across three wavelength bands (2.55–2.68, 2.71–2.87, and 2.79–2.96 eV) using a Hamamatsu streak camera with a resolution of 15 ps. The three adjacent 25-nm ( $\sim 150$  meV)-wide wavelength bands spanned the entire continuous-wave photoluminescence (cw PL) emitted from the QW. Features narrower than 25 nm were resolved by sequentially comparing adjacent 5 or 10 nm data windows offset from each other by 1–4 nm steps. Of course, all TRPL traces represent the sum effect of components with wavelength dependent behavior. However, narrowing the bandwidth of the windows further did not significantly improve the ability to measure wavelength dependence because of the reduced signal-to-noise ratio, especially on the silvered side.

An example of a TRPL trace is presented in Fig. 2(a),

comparing the temporal decay of the unsilvered and silvered QW PL for a 25-nm-wide wavelength band. The luminescence decay constants from the silvered and unsilvered sides were independently derived from exponential fits to the data (5 or 10 nm windows) and then compared under identical pump and detector parameters. The uncertainty in fitted rate constants for a 10 nm window is 2%–5% at wavelengths near the peak cw PL emission (2.75 eV) and rises to as much as 10%–16% at longer and shorter wavelength extremes where the emission is weaker.

On the unsilvered side, the QW exhibited a long single exponential decay whose decay constant  $\tau_0$  was the slowest ( $\tau_0 = 25$  ns) at wavelengths near the peak PL emission (2.76 eV) [Fig. 2(b)]. This very long decay constant, and the correspondingly high PL intensity, indicates a high internal quantum efficiency and insignificant nonradiative processes compared to radiative recombination ( $1/\tau_0 = 1/\tau_{nr} + 1/\tau_r \approx 1/\tau_r$ ).<sup>16,17</sup> Away from the peak PL emission wavelength, the recombination rate accelerates ( $\tau_0 = 4$ –5 ns) at the longest and shortest wavelengths measured. The wavelength dependence of InGaN QW emission has been studied previously,<sup>17</sup> and has been found to differ markedly from the SE rate of a dipole radiator (dipole moment  $d$ ) in a dielectric medium (index of refraction  $n$ )

$$\frac{1}{\tau_r(\omega)} = \frac{4nd^2\omega^3}{3\hbar c^3}, \quad (3)$$

especially at low frequency where shallow level traps, impurities, and quantum-dot-like structures in the QW contribute to recombination. A phenomenological estimate is a Lorentzian

$$\frac{1}{\tau_0(\omega)} \approx \frac{1}{\tau_r(\omega)} = \frac{1}{\tau_0} \frac{\Delta\omega^2}{(\omega - \omega_c)^2 + \Delta\omega^2}, \quad (4)$$

whose peak at ( $\omega_c$ ) and linewidth  $\Delta\omega$  also roughly coincide with that of the measured cw PL [Fig. 2(b)].

By contrast, the weaker PL intensity through the silver-coated surface exhibits a biexponential decay. The slower TRPL relaxation component has a decay constant ( $\tau_2$ ) of between 5–10 ns for emission between 2.61–2.94 eV. The decay constant shows no systematic variation with changing emission wavelength and silver thickness. Regarding the latter, the degree of coupling to the SP mode will be shown to depend on the thickness of the silver film. Comparison of the

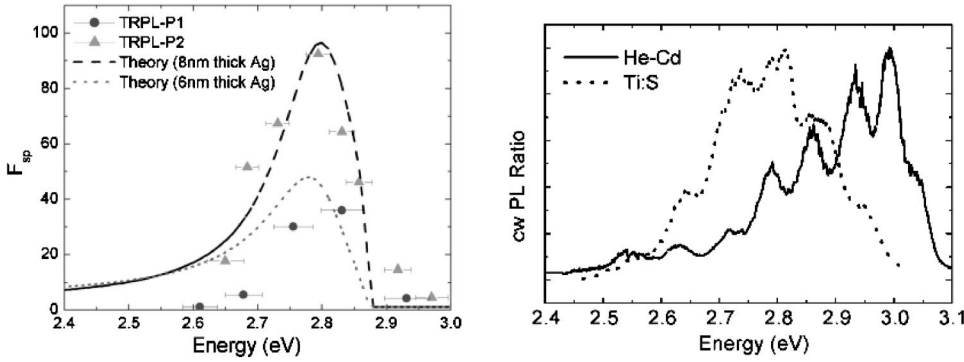


FIG. 3. (a) The Purcell enhancement factor,  $F_{sp}$ , measured using TRPL windows 10 nm (position  $P_1$ ) and 5 nm (position  $P_2$ ) wide. Overlaid is the prediction of the enhancement. (b) Comparison of the time-integrated PL emission ratios for excitation by HeCd and Ti:s lasers. (The undulations in the cw PL arise from interference in the sample.)

relative cw PL intensities of the InGaN reference layers reveals small variations in the thickness of the silver film. (It is thicker at location  $P_2$  than at  $P_1$ .) The fact that  $\tau_2$  is insensitive to these thickness variations suggests that the slowly decaying emission must arise from sources uncoupled to the surface plasmon mode, such as impurity bound excitons of shallow level defect states in GaN layers.

The faster decay component, with decay constant  $\tau_1$ , instead depends sensitively on the thickness of the silver coating and therefore corresponds to enhanced recombination in the QW mediated by the SP mode ( $1/\tau_1 = 1/\tau_{nr} + 1/\tau_r + 1/\tau_{sp} \approx 1/\tau_{sp}$ ). The measured  $\tau_1$  was observed to vary with sample thickness from 235 ps at  $P_2$  to 512 ps at  $P_1$ . As expected, this faster component is strongest near  $E_{sp}$  (2.85 eV). However, the SP resonance is fairly broad because it is evident at energies 200 meV lower than  $E_{sp}$ , and it decays with a time constant almost independent of the emission wavelength. To summarize the wavelength dependence of the SP enhancement, Fig. 3 plots the Purcell factor ( $F_{sp} = 1 + \tau_0/\tau_1$ ) derived from the measured TRPL decay constants. The data demonstrate a sudden rise at higher energies, a peak enhancement near 2.8 eV, and weaker enhancement at lower energies. The maximum values of  $F_{sp}$  were 36 (at 2.83 eV) and 92 (at 2.79 eV) at sample positions  $P_1$  and  $P_2$ , respectively.

Fermi's golden rule (1) provides insight into the frequency dependence of the Purcell factor and reveals the sensitivity of  $F_{sp}$  to the silver thickness  $t$  and Ag-QW separation  $a$ .<sup>11</sup> First, the electric field of the SP mode at the QW must be calculated and used to derive the dipole matrix element. The SP electric field varies only in the  $z$  direction, so the normalization of  $E(z)$  to a half quantum of zero-point fluctuation in the dispersive medium becomes

$$\alpha^2 = \frac{S}{A} = \frac{\hbar\omega/2}{\frac{A}{8\pi} \int_{-\infty}^{\infty} dz \frac{\partial(\omega\varepsilon(\omega,z))}{\partial\omega} |E(z)|^2}, \quad (5)$$

where  $E(z)$  is the un-normalized electric field at a distance  $z$  from the Ag-GaN interface,  $|\alpha E(a)|^2$  is the normalized electric field at QW depth  $a$ ,  $A$  is the quantization area, and  $\varepsilon(\omega,z)$  is the dielectric function of the GaN, Ag, or air. The enhanced recombination rate ( $1/\tau_{sp}$ ) can then be estimated in the QW under the influence of the local electric field from the tangential SP mode

$$\begin{aligned} \frac{1}{\tau_{sp}(\omega)} &= \frac{2\pi}{\hbar} \left[ \frac{1}{3} d^2 |\alpha E(a)|^2 \right] 2\pi k \frac{A}{(2\pi)^2} \frac{dk}{d(\hbar\omega)} \\ &= \frac{S}{3\hbar^2} |dE(a)|^2 k \frac{dk}{d\omega}, \end{aligned} \quad (6)$$

where the factor 1/3 comes from spatial averaging of polarization. Inserting measured values for  $a$  (12 nm) and  $t$  (8 nm) while using the  $\tau_1$  data to fit for  $d$  (24 nm), the calculation predicts that  $\tau_{sp}$  should be relatively independent of frequency from 2.6 eV to  $E_{sp}$ .

The frequency dependence of  $F_{sp}$  derives from Eq. (6) and the frequency dependence of the unsilvered QW recombination rate  $\tau_0$  [Fig. 2(b)]. For the parameters in this experiment, the frequency dependence of  $F_{sp}$  below  $E_{sp}$  derives primarily from  $\tau_0$ . Unfortunately, a predictive theory of the  $\tau_0$  is not available, so an accurate estimate of  $F_{sp}$  is not possible. However, if Eqs. (4) and (6) are used as approximations for  $\tau_0$  and  $\tau_1$ , respectively, then  $F_{sp}(\omega) \approx 1 + \tau_0/\tau_1$  may be plotted (Fig. 3) using the parameters for this sample. The predicted frequency peak and width of  $F_{sp}$  agree well with the measured peaks and widths of the TRPL data. The peak value of  $F_{sp}$  is a sensitive function of Ag thickness through  $\tau_{sp}$ . A reduction of  $t$  from 8 to 6 nm halves the peak value of  $F_{sp}$ , suggesting that the differing values of  $F_{sp}$  observed at  $P_1$  and  $P_2$  arise from small variations of the Ag thickness.

Recently,  $F_{sp}$  was measured in a similar sample by means of cw PL using a HeCd excitation source ( $E_{ex} = 3.82$  eV,  $\lambda_{ex} = 325$  nm).<sup>11</sup> A ratio of the PL emission for the unsilvered to silvered sides was measured as a function of wavelength, and a peak enhancement factor of 55 was estimated from the data. Those measurements were repeated here, and although the measured enhancement factors were similar to and consistent with the TRPL data, the energy of maximum enhancement in both cw PL measurements was blue shifted from  $E_{sp}$ . When time-integrated PL is measured using the Ti:S laser instead, this blueshift disappears (inset, Fig. 3). Note that the HeCd laser excites all layers of the sample while the Ti:S laser only excites the QW and GaN defects. Therefore, any cw PL ratio measured using a HeCd laser must be understood to represent  $F_{sp}$  convolved with other excitation-dependent effects (particularly in the cap layer), while the TRPL data measures only  $F_{sp}$ . Furthermore, the role of nonradiative recombination was ignored in

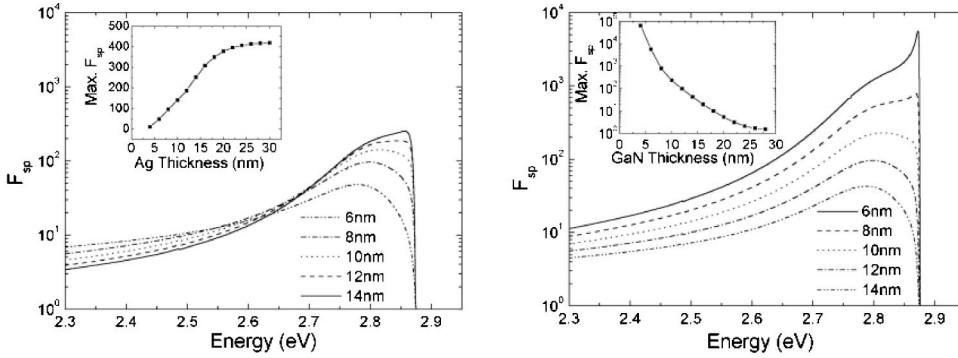


FIG. 4. (a) Calculated  $F_{sp}$  for various Ag thicknesses  $t$  with Ag-QW separation  $a = 12$  nm. Inset: Maximum  $F_{sp}$  values for a given  $t$  with  $a = 12$  nm. (b) Calculated  $F_{sp}$  for various Ag-QW separations  $a$  with Ag thickness  $t = 8$  nm. Inset: Maximum  $F_{sp}$  values for a given  $a$  with  $t = 8$  nm.

that work, leading to an overly simplistic estimate of  $F_{sp}$  based on Eq. (3). The phenomenological estimate (4) includes both radiative and nonradiative effects.

Using Eqs. (4) and (6) to estimate  $F_{sp}$ , even larger enhancements are predicted over narrower frequency bands. For a prominent resonance in  $F_{sp}$ , Fig. 4 indicates that it is necessary for the Ag film to possess a thickness  $\geq 6$  nm for a QW 12 nm from the surface. In support of the earlier deduction that the Ag film is slightly thicker at  $P_2$  than  $P_1$ , the value of  $F_{sp}$  is predicted to increase with increasing film thickness and asymptotically approaches 422 for  $t \geq 26$  nm ( $a = 12$  nm).

The strength and frequency dependence of  $F_{sp}$  are even more sensitive functions of the Ag-QW separation, especially for small  $a$ . Resonant enhancements of more than  $10^4$  are

predicted for QW's only 4 nm below the surface. These predicted enhancements may actually be conservative because the synergistic "back action" coupling between dipole emitters and SP field, which increases as  $a$  decreases, is not included in this calculation. A more comprehensive calculation of this enhancement factor, including the necessary radiation reaction effects, is beyond the scope of this paper. Nevertheless, the enhancement will likely remain broad because inhomogeneous broadening ( $\hbar \Delta \omega_{inh} \approx 100$  meV) will probably limit  $\omega_c / \Delta \omega < 30$ .

The authors would like to thank S. Kellar, U. Mishra, and S. DenBaars of UCSB for providing the QW sample, and I. Gontijo, M. Boroditsky, and G. Khitrova for useful discussions. This work was supported by the Army Research Office and the National Research Council.

\*Email address: arup@phy.duke.edu

<sup>1</sup>E.M. Purcell, Phys. Rev. **69**, 681 (1946).

<sup>2</sup>E.V. Goldstein and P. Meystre, in *Spontaneous Emission and Laser Oscillation in Microcavities*, edited by H. Yokoyama and K. Ujihara (CRC, Boca Raton, 1995), p. 1.

<sup>3</sup>S.M. Dutra and P.L. Knight, Phys. Rev. A **53**, 3587 (1996).

<sup>4</sup>C. Weisbuch, H. Benisty, and R. Houdré, J. Lumin. **85**, 271 (2000).

<sup>5</sup>J.M. Gérard *et al.*, Phys. Rev. Lett. **81**, 1110 (1998); E. Moreau *et al.*, Appl. Phys. Lett. **79**, 2865 (2001).

<sup>6</sup>J. Vučković, M. Lončar, and A. Scherer, IEEE J. Quantum Electron. **36**, 1131 (2000).

<sup>7</sup>M. Borditsky *et al.*, J. Lightwave Technol. **17**, 2096 (1999).

<sup>8</sup>T. Baba *et al.*, J. Lightwave Technol. **17**, 2113 (1999).

<sup>9</sup>N.E. Hecker *et al.*, Appl. Phys. Lett. **75**, 1577 (1999).

<sup>10</sup>T. Baba *et al.*, Jpn. J. Appl. Phys. **35**, 97 (1996).

<sup>11</sup>I. Gontijo *et al.*, Phys. Rev. B **60**, 11 564 (1999).

<sup>12</sup>A. Brillante and I. Pockran, J. Mol. Struct. **79**, 169 (1982).

<sup>13</sup>S. Kellar *et al.*, J. Cryst. Growth **195**, 258 (1998), and references therein.

<sup>14</sup>H. Ehrenreich and H.R. Philipp, Phys. Rev. **128**, 1622 (1962); A. Liebsch, Phys. Rev. Lett. **71**, 145 (1993).

<sup>15</sup>G. Hass and L. Hadley, *American Institute of Physics Handbook*, 3rd ed. (McGraw-Hill, New York, 1972), Chap. 6g, pp. 6–149; D. Brunner *et al.*, J. Appl. Phys. **82**, 5090 (1997).

<sup>16</sup>B. Monemar *et al.*, Proc. SPIE **3624**, 168 (1999).

<sup>17</sup>S. F. Chichibu, Y. Kawakami, and T. Sota, in *Introduction to Nitride Semiconductor Blue Lasers and Light Emitting Diodes*, edited by S. Nakamura and S. F. Chichibu (Taylor & Francis, London, 2000), Chap. 5, pp. 153–270, and references therein.